Available online at www.sciencedirect.com
SCIENCE DIRECT®
Journal of the European Ceramic Society 26 (2006) 161–167
www.elsevier.com/locate/jeurceramsoc

Sintering mechanism and ceramic phases of an illitic–chloritic raw clay

A. Khalfaoui, S. Kacim, M. Hajjaji*

Laboratoire de Chimie Physique, Département de Chimie, Faculté des Sciences Semlalia, Université Cadi Ayyad, B.P. 2390, Marrakech, Morocco

Received 30 June 2004; received in revised form 12 October 2004; accepted 24 October 2004
Available online 30 December 2004

Abstract

Sintering process and ceramic phases of a non-calcareous illitic–chloritic clay were investigated in the range 850–1075 °C by means of X-ray diffraction (XRD), thermal analysis, scanning electron microscopy and energy dispersive X-ray spectrometry as well as by measuring some firing characteristics. It is found that the sintering mechanism is mainly governed by viscous flow and the activation energy turns around 100 kJ/mol.

Moreover, it is evidenced that firing characteristics are principally controlled by the glassy phase formation. On the other hand, it is observed that magnesium is the most active element in the neoformation process, and Mg-spinels, olivine and enstatite were the main neocrystallized phases. The formation of the latter magnesian phases was discussed on the basis of the $MgO–SiO_2–Al_2O_3$ phase diagram. It derived that a part of free silica is involved in the precipitation of Mg-phases.
© 2004 Elsevier Ltd. All rights reserved.

Keywords: Sintering; Microstructure-final; Clays; Traditional ceramics

1. Introduction

Firing transformations of non-calcareous clays, containing micaceous mineral and kaolinite associated with quartz, hematite and feldspars have been extensively investigated (e.g.[1–6]). Spinels (γ-Al_2O_3, $MgAl_2O_4$), glassy phase, K-feldspar and mullite are the common neoformed phases. However, disparities are reported in terms of the origin of some neocrystallized phases, such as mullite and spinels. Moreover, the prediction of ceramic phases, basing on the known equilibrium diagrams, are rarely achieved, because of the presence of mineralizers, the complexity of the chemical compositions of raw clays, the effects of firing and processing conditions, and because of the equilibrium state is seldom reached.

If firing transformations of kaolinitic–illitic clays or individual clay minerals (kaolinite, illite) have been the subject of numerous studies, a little attention has been paid to the study of transformations of raw clays containing mica/illite, kaolinite and chlorite.[7–9] Thereby, this study is devoted to the sintering mechanism and ceramic phases of a non-calcareous clay, containing illite, chlorite and kaolinite. For these purposes, firing characteristics (shrinkage, water absorption and mechanical strength) were measured and the neomineralization processes were investigated principally by X-ray diffraction (XRD), thermal analysis, scanning electron microscopy and energy dispersive X-ray spectrometry.

2. Materials and methods

The studied clay is from a Triassic deposit located at Al Haouz (Morocco). It consists of ∼22 wt.% quartz, ∼8 wt.% hematite and phyllosilicates (∼40 wt.% illite, ∼15 wt.% chlorite and ∼5 wt.% kaolinite). The balance is mainly formed of K-feldspar.

The chemical compositions of the raw clay and its <2 μm fraction are given in Table 1.

For firing tests, bars of 4 mm × 10 mm × 40 mm were prepared by extrusion from a dough, containing an optimum amount of water (26 wt.%). The extruded bars were kept at

* Corresponding author. Fax: +212 44 37408.
E-mail address: hajjaji@ucam.ac.ma (M. Hajjaji).

0955-2219/$ – see front matter © 2004 Elsevier Ltd. All rights reserved.
doi:10.1016/j.jeurceramsoc.2004.10.030

Table 1
Chemical compositions of the raw clay (C) and its <2 μm fraction (F)

	SiO_2	Al_2O_3	Fe_2O_3	MgO	CaO	K_2O	Na_2O	TiO_2	MnO	LOI[a]
C	50.8	19.2	9.4	4.3	0.3	4.3	1.6	0.8	0.1	8
F	47.6	22.5	11.7	4.6	0.2	4.8	0.1	0.8	0.1	7

[a] Loss on ignition at 1000 °C.

room temperature for 1 day and oven-dried at 100 °C for 24 h. The as-dried samples were fired for 2 h at maximum temperatures ranging from 850 to 1075 °C, in an electric furnace operating under static air. The average heating rate, up to the maximum firing temperature, is 20 °C/min.

Firing technological properties (linear shrinkage (λ), water absorption (WA) and bending strength (σ)) were measured. λ and WA were evaluated according to the procedures reported in.[10] σ was determined with the 3-points technique, using a EX 150 DeltaLab apparatus. The microstructural changes of fired samples were investigated by means of a PHILIPS X'Pert MPD X-ray diffractometer, operating with a copper anticathode as well as by a JEOL JMS 5500 scanning electron microscope (SEM) apparatus, equipped with a Falcon EDAX system. Concerning the X-ray diffraction, randomly oriented samples were analyzed under the following conditions: generator voltage, 40 kV; tube current, 30 mA; scan step size, 0.05°; time/step, 0.5 s. SEM examinations were carried out on freshly fractured shards, which were covered with carbon. The maximum resolution turns around 3.5 nm. The elemental quantitative analyses were performed by EDAX technique, without standards (ZAF method).

Firing transformations were also followed by thermal analysis using a Rheometric Scientific STA 1500 apparatus, operating under N_2 atmosphere with a heating rate of 20 °C/min. The glassy phase content was evaluated by chemical etching, using a boiled alkaline solution (5 wt.% NaOH).

3. Results and discussion

3.1. Sintering mechanism

In Fig. 1, a typical curve of the isothermal linear shrinkage (λ) as a function of the soaking time (t) is given. In the same figure, $t\lambda^{-1}$ versus time is reported. Based on the results reported in,[11] the linear evolution of $t\lambda^{-1} = f(t)$, which is observed only for 950 and 1000 °C, shows that the sintering mechanism proceeds mainly by melt flow.[12] This result is supported by the quantitative amount of the glassy/amorphous phase developed with increasing firing temperature (Fig. 2). The significant development of melt, which is theoretically expected since the ratio $(Na_2O + K_2O)/(CaO + MgO)$ exceeds 1,[13] has a marked impact on the firing characteristics (Fig. 3): because of the melt flow for $T > 900$ °C, the open porosity and consequently water absorption experienced a drastic decrease, whereas the mechanical strength as well as shrinkage increased. In this connection, it is established that the bending strength (σ) and

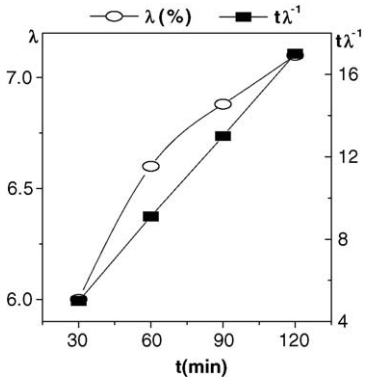

Fig. 1. Typical curve of the isothermal linear shrinkage as a function of firing time ($T = 950$ °C).

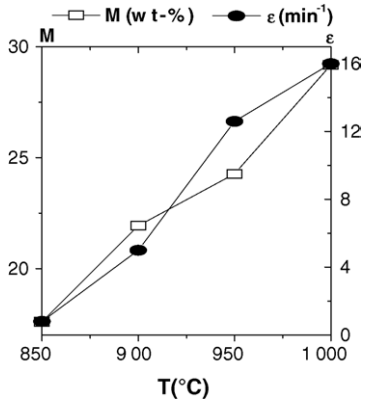

Fig. 2. Evolutions of the melt content (M) and rate of increase of viscosity (ε) vs. firing temperature.

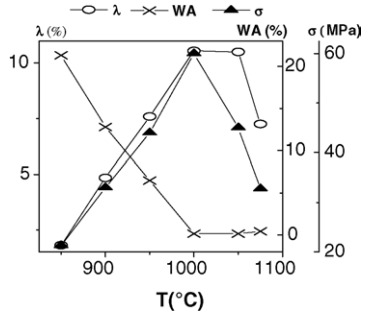

Fig. 3. Variation of technological properties of fired samples as a function of firing temperature (λ: linear shrinkage; WA: water absorption; σ: mechanical strength).

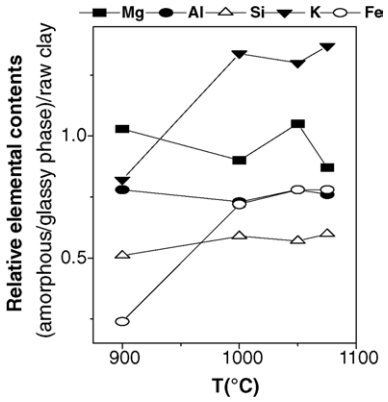

Fig. 4. Evolution of the amounts of the major elements in the amorphous/glassy phase with reference to those in the raw clay as a function of firing temperature.

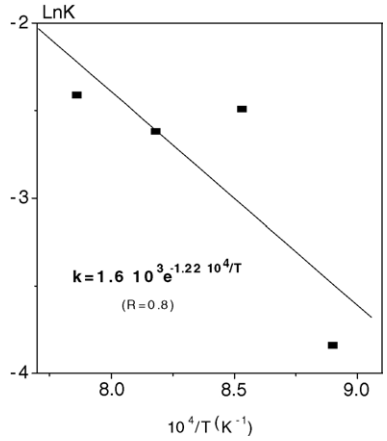

Fig. 5. Evolution of the kinetic constant against firing temperature.

shrinkage depend on the melt content (M in wt.%) according to the relations:

$$\sigma = 4.83\,M - 65.37; \quad \lambda = 0.77\,M - 11.74$$

The rate of increase of the melt viscosity (ε) was evaluated from the ratio $\varepsilon = \beta/\alpha$, where α^{-1} and β^{-1} are the limit of shrinkage after an infinite time and the initial shrinkage rate, respectively.[11] As shown in Fig. 2, ε increased with firing temperature, likely because of phases neoformation, which happened beyond 900 °C, and/or of the chemical composition change of the liquid phase. To check the latter assumption, the chemical composition of the amorphous/glassy phase, which is developed at different firing temperatures, was followed by energy dispersive X-ray spectrometry. As can be seen in Fig. 4, the relative chemical compositions of K and Fe increased for up to 1000 °C, whereas the contents of Mg, Al and Si are quasi-constant. It may be noticed that the amounts of the two latter elements are close to those of Al and Si of illite (∼40 wt.%). Presumably, the illite breakdown products constituted a framework for the viscous phase, and the liquid K-enrichment led to the formation of Al–Si–O complexes, which should increase the melt viscosity, as reported in [14].

Referring to the kinetics data reported in Fig. 1, shrinkage versus time obeys a parabolic law: $\lambda^2 = 2kt + \text{constant}$, where k is the kinetic constant. Based on the Arrhenius equation ($k = A\exp(-E_a/RT)$; A is the frequent factor and E_a the energy of activation) and the evolution of Lnk as a function of the reciprocal firing temperature (Fig. 5) the activation energy turns around 100 kJ/mol. Likely because of the implication of different activated phenomena (pores elimination and/or coalescence, species diffusion, melt formation, phase dissolution) the correlation factor is not close to unity.

3.2. Phases transformations

Typical X-ray diffraction patterns of fired clay samples are given in Fig. 6. An overall examination shows that firing at 900 °C induced the breakdown of kaolinite and chlorite, as commonly reported (e.g.[3,15]), but quartz, hematite, K-feldspar and illite were slightly affected. For further heating to 950 °C, peaks of illite vanished, except that located at 19.72° (2θ). Moreover, reflections which are assignable to a spinel-type phase, likely γ-Al_2O_3 or Al–Si spinel, manifested. Referring to the result of the thermal analyses of the raw clay (Fig. 7), this spinel, which is accompanied by an exothermic effect, developed nearby 925 °C. Likely because of its tiny size, the SEM examinations did not allow to identify this phase. As the firing temperature increased to 1000 °C, the original K-feldspar became well crystallized and a set of spinels, with close lattice parameters, developed. Apparently, these spinels occurred as a fine precipitation within the amorphous/glassy phase, which is manifested as extended featureless zones (Fig. 8). Firing at 1050 and 1075 °C led to the formation of olivine (Mg, $Fe)_2SiO_4$ and two magnesian spinels which can by identified as: ($Mg_{0.73}Al_{0.27}$)($Al_{0.865}$

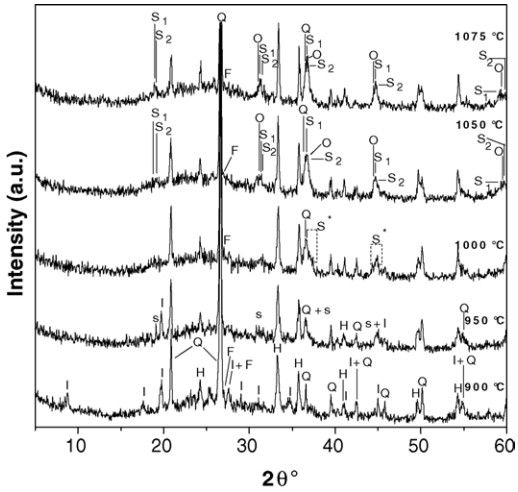

Fig. 6. X-ray diffractograms of raw clay samples fired at different temperatures. I: illite; Q: quartz; H: hematite; F: K-feldspar; s: spinel-type phase; S^*: set of Mg-spinels; S_1: spinel ($Mg_{0.73}Al_{0.27}$)($Al_{0.865}$ $Mg_{0.135}$)$_2O_4$; S_2: spinel ($MgAl_2O_4$); O: olivine.

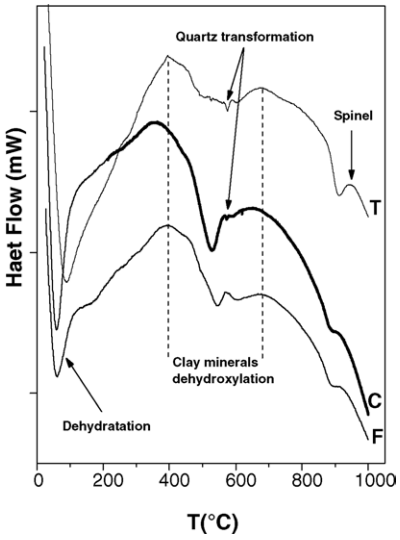

Fig. 7. Thermograms of raw clay (C), <2 μm fraction (F) and acid-etched raw clay (T).

$Mg_{0.135})_2O_4$ (JCPDS file 86-0089) and $MgAl_2O_4$. Scarce precipitation of enstatite (Fig. 9) and calcic-aluminosilicates, presumably clinopyroxenes (Fig. 10) was evidenced by SEM.

A careful observation of the above X-ray diffractograms (Fig. 6) showed that some reflections of quartz exhibited a splitting for $T > 1000\,^{\circ}C$. This splitting may be taken as an indication of the presence of a chemically modified and native quartz: the former quartz consists of the outer zones of the free silica coarse particles, which are a subject of elemental diffusion, whereas the original quartz corresponds to the core of the coarse particles. In such conditions, the lattice parameters of both quartz should be slightly different. As far as quartz modification is concerned, Laczka ([16]) reported that Al or alkalis insertion into the quartz lattice may happen and the substituted quartz should lead to the formation of a transition phase, which is in its turn transformed into melt. Thus, transformation of quartz into cristobalite could not occur.

In Fig. 11, the relative X-ray intensity of the (1 0 0) reflection of quartz as a function of the firing temperature is plotted. Globally, three domains are distinguished. The intensity decrease observed in the range 850–900 °C may be attributed to the disappearance of tiny grains of quartz, which are associated with the <2 μm clay fraction. The almost constancy of the relative intensity, which is manifested between 900 and 950 °C, may be taken as an incubation period for the reactivity of coarse grains of quartz, which became well marked at 1000 °C. Apparently, the above mentioned quartz modification happened upon this stage.

Referring to the results reported in,[17] olivine, enstatite and spinel ($MgAl_2O_4$) should be derived from the thermal decomposition of chlorite. To evidence the implication of chlorite in the crystallization process of the latter magnesian phases, samples of acid-etched clay, which are exempt of

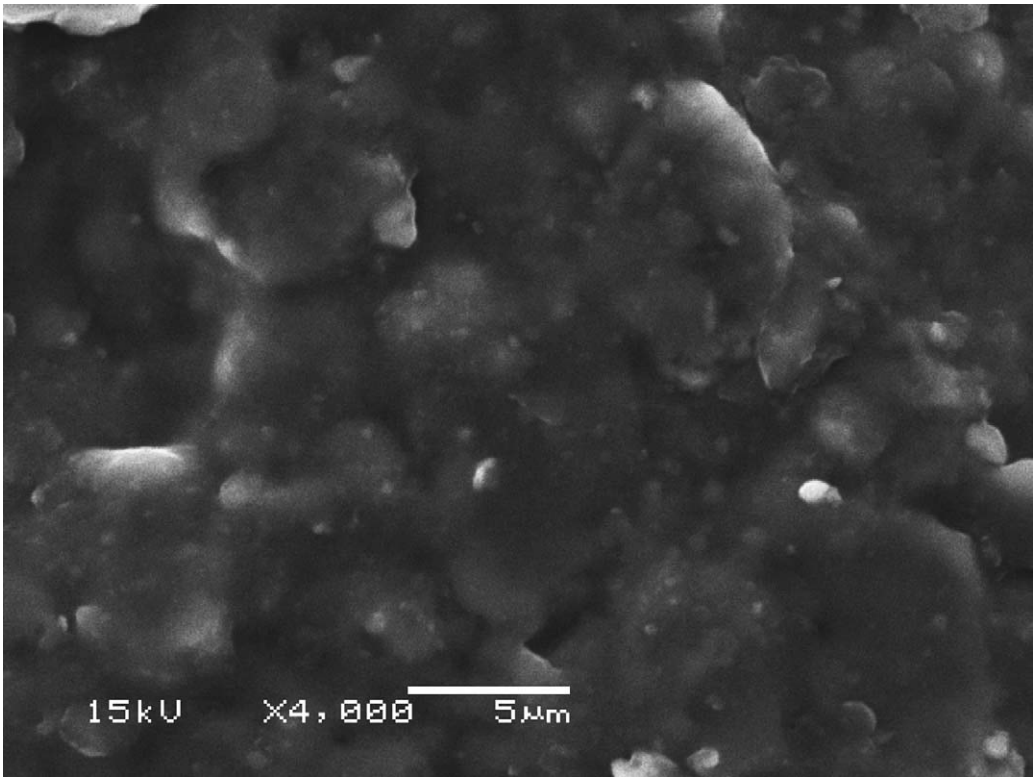

Fig. 8. Scanning electron micrograph showing fine precipitation within the amorphous/glassy phase formed at 1000 °C.

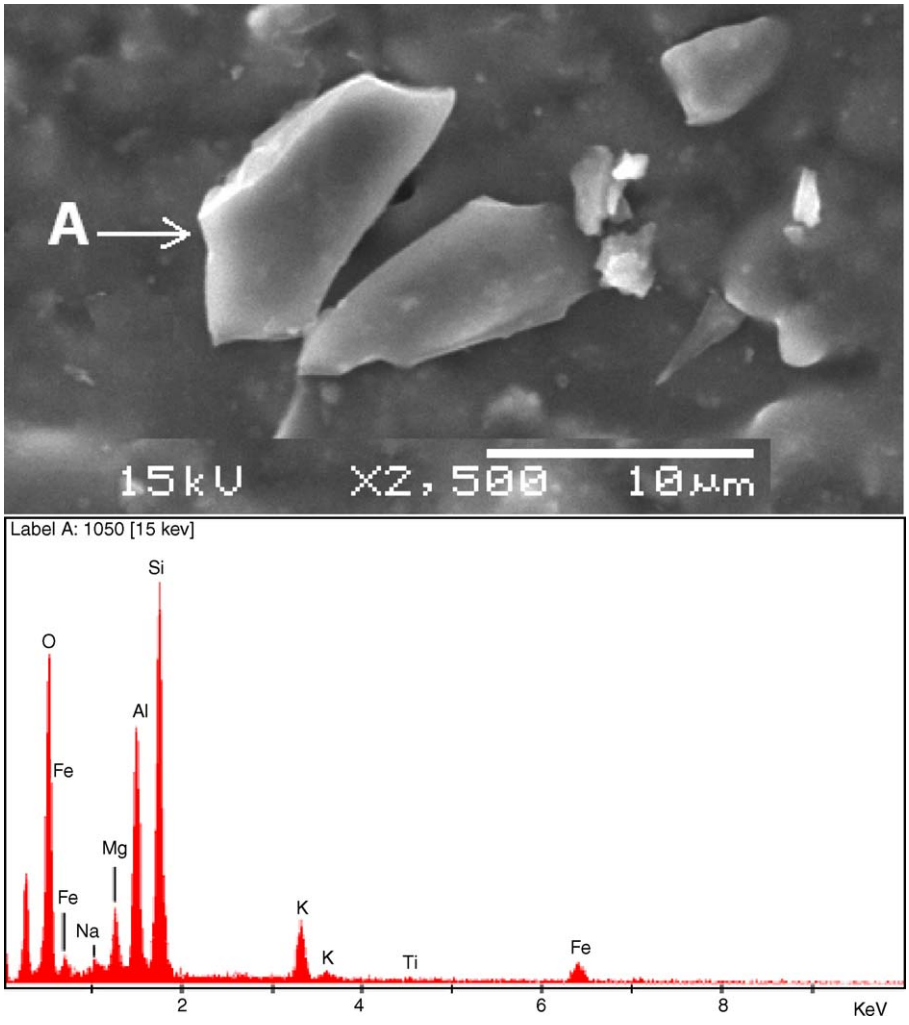

Fig. 9. Scanning electron micrograph and EDX spectrum of enstatite (A).

hematite and chlorite, were fired at 1050 °C and examined by XRD (Fig. 12). It is found that olivine and Mg-spinels were developed, but their contents were less important. This result suggests that a part of Mg derived from illite, which is the major clay mineral constituent of the acid-treated clay samples.

It should be noticed that the above observed formation sequence of the magnesian phases, i.e., spinel, olivine/forsterite and enstatite/pyroxene, is not the same as that reported in,[17] namely forsterite, spinel and enstatite. This difference may be explained by the fact that, in the case of the studied clay, Mg in the brucite layer of chlorite is partially substituted by Al. In such condition, the formation of $MgAl_2O_4$ is favored as compared with that of Mg_2SiO_4.

It is worth noting that mullite, which is developed in fired illitic–chloritic clays,[9] was not detected, in spite of the presence of its precursor (spinel-type phases).[18–20] Presumably, its absence is due to the high amount of Mg and/or to the melt aggressivety,[21] or because its amount is below the X-ray detection threshold.

To determine the origin of the spinel-type phase, samples of raw clay, clay-sized fraction (<2 μm) and acid-etched raw clay were thermally analyzed. As can be seen in Fig. 7, the exotherm associated with this spinel is much intense for the illite rich sample, i.e., the acid-treated raw clay. Thus, it may be deduced that this phase is originated from the breakdown of illite.

In view of the above results, it may be outlined that potassium is almost involved in the melt development and magnesium is mainly implicated in the occurrence of spinels, olivine and enstatite. Because of the crystallization of the latter magnesian compounds, prediction attempts of the neoformed phases was done on the basis of $MgO–SiO_2–Al_2O_3$ equilibrium diagram. As can be deduced from Fig. 13, both compositions of the raw clay and its <2 μm fraction should lead to cordierite, enstatite and silica, instead of spinels, enstatite and olivine. Apparently, such difference is not related to the equilibrium state, since the mineralogical compositions of compacted and extruded raw clay samples, which were fired at 1000 and 1050 °C for 2

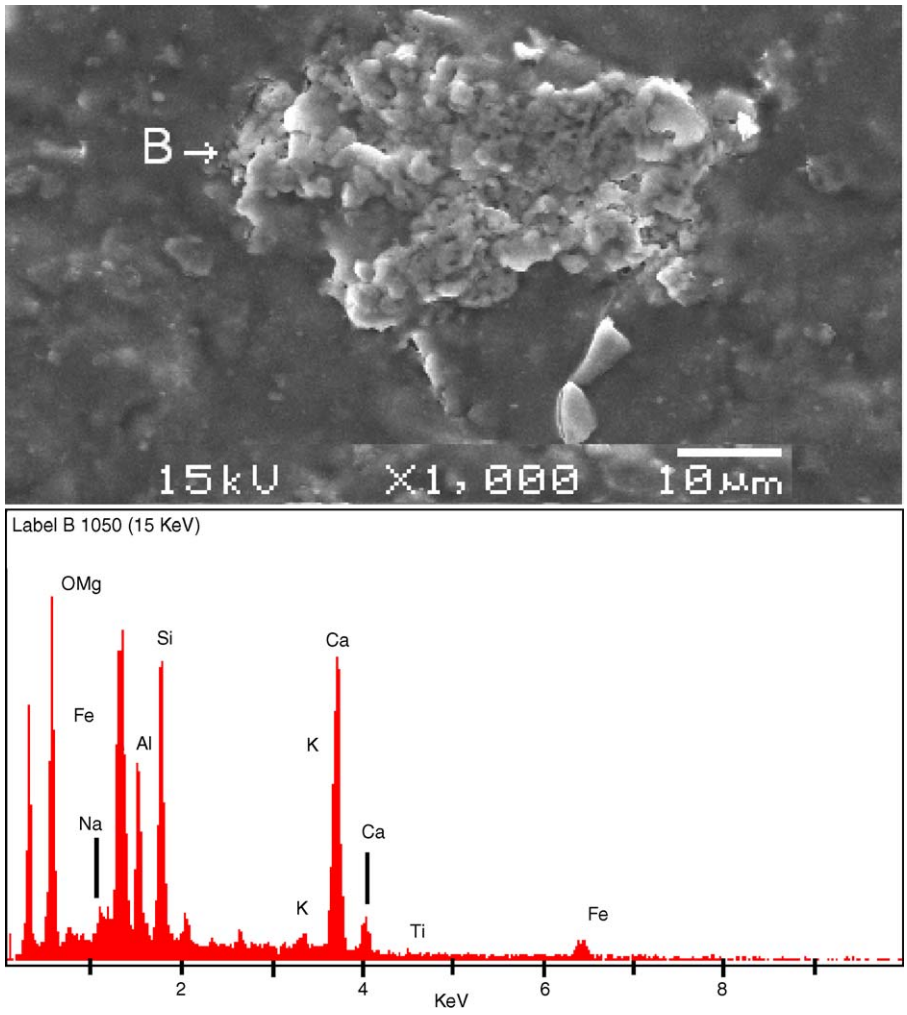

Fig. 10. Scanning electron micrograph and EDX spectrum of calcic-aluminosilicate phase (B).

and 24 h, respectively, were similar. As far as the phases formation is concerned, it appears that a part of quartz, whose activity increased with increasing firing temperature, participated in the Mg-phases formation and consequently the precipitation sequence followed the direction shown in Fig. 13.

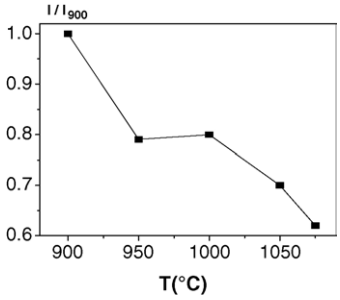

Fig. 11. Evolution of relative X-ray intensity of (1 0 0) reflection of quartz as a function of firing temperature. I_{900}: X-ray intensity of quartz in raw clay sample fired at 900 °C.

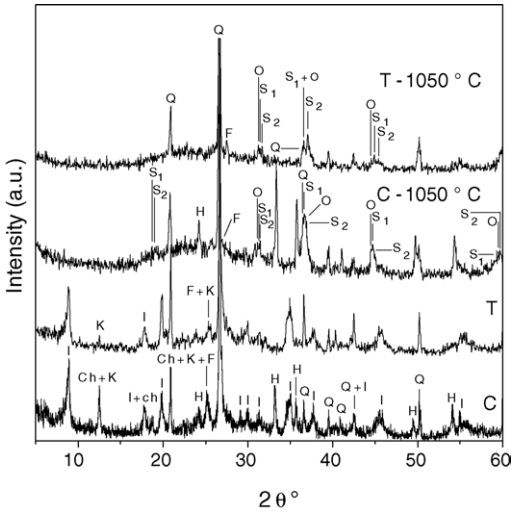

Fig. 12. X-ray diffraction patterns of raw clay (C) and acid-etched raw clay (T) samples taken in the crude and fired states. I: illite; Ch: chlorite; K: kaolinite; Q: quartz; H: hematite; F: K-feldspar; S_1: spinel $(Mg_{0.73}Al_{0.27})(Al_{0.865}Mg_{0.135})_2O_4$; S_2: $MgAl_2O_4$; O: olivine.

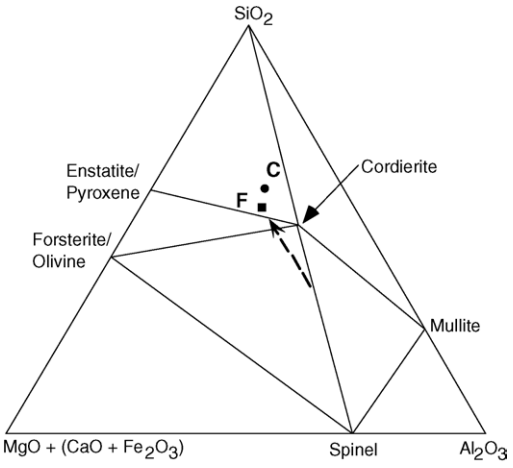

Fig. 13. $MgO–SiO_2–Al_2O_3$ phase diagram. C and F are the representative points of the chemical compositions of the raw clay and its <2 μm fraction, respectively. (⟶) represents the direction of Mg-phases occurrence sequence with increasing firing temperature.

4. Conclusions

1. The melt flow, which is mainly originated from the breakdown of illite, played a chief role in the sintering process and controlled the firing characteristics.
2. Free silica experienced a partial chemical modification and contributed to the Mg-phases crystallization process. The bonded silica is mainly involved in the melt development.
3. Potassium, which is mainly supplied by illite, was implicated in the liquid formation, whereas magnesium, which is derived either from illite and chlorite, was involved in the crystallization of the magnesian phases, namely Mg-spinels, olivine and enstatite.
4. The difference between the predicted and observed mixtures of phases is partly due to the gradual reactivity of free silica.

References

1. González-García, F., Romero-Acosta, V., García-Ramos, G. and González-Rodríguez, M., Firing transformations of mixtures of clays containing illite, kaolinite and calcium carbonate used by ornamental tile industries. *Appl. Clay Sci.*, 1990, **5**, 361–375.
2. Dubois, J., Murat, M., Amroune, A., Carbonneau, X. and Gardon, R., High-temperature transformation in kaolinite: the role of crystallinity and firing atmosphere. *Appl. Clay Sci.*, 1995, **10**, 187–198.
3. Parras, J., Sánchez-Jiménez, C., Rodas, M. and Luque, F. J., Ceramic applications of Middle Ordovician shales from central Spain. *Appl. Clay Sci.*, 1996, **11**, 25–41.
4. Riccardi, M. P., Messiga, B. and Duminuco, P., An approach to the dynamics of clay firing. *Appl. Clay Sci.*, 1999, **15**, 393–409.
5. Hajjaji, M., Kacim, S. and Boulmane, M., Mineralogy and firing characteristics of a clay from the valley of Ourika (Morocco). *Appl. Clay. Sci.*, 2002, **21**, 203–212.
6. Aras, A., The change of phase composition in kaolinite- and illite-rich clay-based ceramic bodies. *Appl. Clay. Sci.*, 2004, **24**, 257–269.
7. Fabbri, B. and Fiori, C., Clays and complementary raw materials for stoneware tiles. *Miner. Petrogr. Acta*, 1985, **29-A**, 535–545.
8. Fiori, C., Fabbri, B., Donati, G. and Venturi, I., Mineralogical composition of the clay bodies used in the Italian tile industry. *Appl. Clay Sci.*, 1989, **4**, 461–473.
9. Sánchez-Soto, P. J., Díaz-Hernández, J. L., Raigón-Pichardo, M., Ruiz-Conde, A. and García-Ramos, G., Ceramic properties of a spanish clay containing illite, chlorite, and quartz. *Br. Ceram. Trans.*, 1994, **93**, 196–201.
10. Dondi, M., Marsigli, M. and Venturi, I., Firing behaviour of italian clays used in brick and roofing tile production. *Ind. Laterizi.*, 1998, **54**, 382–394.
11. Lemaître, J. and Delmon, B., Study of sintering mechanism of kaolinite at 900 and 1050 °C; influence of mineralizers. *J. Mater. Sci.*, 1977, **12**, 2056–2064.
12. Frenkel, J., Viscous flow of crystalline bodies under the action of surface tension. *J. Phys. (USSR)*, 1945, **9**, 385–391.
13. Segard, G., *Etude de l'expansion d'argiles dans une flamme.*Thèse de 3ème cycle. Université des Sciences et techniques de Lille, France, 1980.
14. Ranogajec, J., Djuric, M., Radeka, M. and Jovanic, P., Influence of particle size and furnace atmosphere on the sintering of powder for tiles production. *Ceram. Silik.*, 2000, **44**(2), 71–77.
15. Jordán, M. M., Boix, A., Sanfeliu, T. and de la Fuente, C., Firing transformations of cretaceous clays used in the manufacturing of ceramic tiles. *Appl. Clay Sci.*, 1999, **14**, 225–234.
16. Laczka, M., The influence of admixtures in natural quartz on its phase transformations. *Silic. Ind.*, 1990, **1-2**, 59–68.
17. Barlow, S. G., Manning, D. A. C. and Hill, P. I., The influence of time and temperature on the reactions and transformations of clinochlore as a ceramic clay mineral. *Int. Ceram.*, 2000, **2**, 5–10.
18. Lemaître, J., Léonard, A. J. and Delmon, B., Le mécanisme de la transformation thermique de la métakaolinite. *Bull. Minér.*, 1982, **105**, 501–507.
19. Murad, E. and Wagner, U., Pure and impure clays and their firing products. *Hyperfine Interact.*, 1989, **45**, 161–177.
20. Murad, E. and Wagner, U., The thermal behaviour of an Fe-rich illite. *Clay Miner.*, 1996, **31**, 45–52.
21. Jund, J., *Etude minéralogique et technique des céramiques de L'Alsace du nord: terre cuite vernissée de Soufflenheim et grés au sel de Betschdorf.* Thesis (thèse de spécialité), Université Louis Pasteur, Strasbourg, France, 1979.